Pressure-Gradient Sorption Calorimetry of Flexible Porous Materials: Implications for Intrinsic Thermal Management

Wesley K. Feldmann,[a] Catharine Esterhuysen,[a] and Leonard J. Barbour*[a]

Thermal management is an important consideration for applications that involve gas sorption by flexible porous materials. A pressure-gradient differential scanning calorimetric method was developed to measure the energetics of adsorption and desorption both directly and continuously. The method was applied to the uptake and release of CO_2 by the well-known flexible metal–organic frameworks MIL-53(Al) and MOF-508b. High-resolution differential enthalpy plots and total integral enthalpy values for sorption allow comprehensive assessment of the thermal behavior of the materials throughout the entire sorption process. During adsorption, the investigated materials display the ability to offset exothermic adsorption enthalpy against endothermic structural transition enthalpy, and vice versa during desorption. The results show that flexible materials offer reduced total integral heat over a working range when compared to rigid materials.

Flexible porous materials potentially offer enhanced working capacities for applications involving the uptake and release of gases.[1,2] The working capacity of a material is also influenced by thermal effects associated with the sorption and desorption processes.[3] For example, since adsorption is exothermic it elevates the sample temperature, which can reduce the total uptake capacity as well as increasing the onset pressure of the gate-opening event.[4,5] Therefore, effective thermal management is critical for the maintenance of working capacities over large loading ranges. This can be assessed by determining the enthalpy changes due to specific events that occur during sorption and desorption. These energetic events (e.g., host-guest and guest-guest interactions, as well as structural changes within the adsorbent) are cumulative and may occur either consecutively or concurrently.[6]

Sorption enthalpies (ΔH) are usually determined using indirect isosteric or direct calorimetric methods. The isosteric method is based on the Clausius-Clapeyron equation and is most commonly applied to materials exhibiting type I sorption profiles.[7–9] However, this method is not usually applied to materials exhibiting stepped or type-F profiles[10] due to sorption-induced structural changes; we note that an adapted approach has been reported by Long and co-workers.[11,12] The isosteric approach is subject to certain assumptions, such as ideal gas behavior[13] and the choice of numerical fitting of the isotherms and isosteres.[14] Many of these issues have been addressed through rigorous derivations, corrections and additions relating to the Clausius-Clapeyron equation.[13–16] Although Grand Canonical Monte Carlo (GCMC) simulations can be used to approximate $-\Delta H_{ads}$ values for flexible materials, accurate results require crystallographic determination of the atomic coordinates both before and after the structural transition. Experimental reference data are often also needed.[17] On the other hand, adsorption calorimetry provides direct quantification of the thermal events associated with the different stages of the sorption process. The enthalpies can be determined at a temperature of choice, thus simulating working conditions and yielding information relevant to practical heat management, i.e. how much cooling is required during adsorption.

An accurate enthalpy profile over the working range of a flexible material enables individual assessment of each of the thermal effects (Figure 1). This allows identification of effects that are unique to flexible materials, such as the potential for intrinsic thermal management.[2,18] An endothermic structural transition has been shown to mitigate exothermic guest adsorption, leading to reduced total heat generation.[2,18] The degree to which the heat may be offset is primarily dependent on the magnitude of the endothermic structural transition[19,20] and the strength of the host-guest interactions.[21]

We recently reported on the use of pressure-gradient differential scanning calorimetry (PG-DSC) to determine enthalpy changes for type I sorption processes over an extended loading range.[25] The advantage of PG-DSC is the gradual introduction/extraction of gas, resulting in maintenance of quasi-equilibrium conditions throughout the experiment.[26] Such conditions improve the resolution of the data and facilitate faster completion times for each experiment.[25] As a logical extension of this work, we now report application of our method to flexible porous materials. The high resolution and continuous data enable identification and quantification of the subtle thermal phenomena[6] associated with

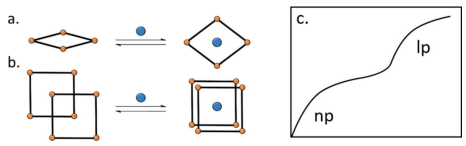

Figure 1. Examples of modes of flexibility:[22] (a) Breathing (e.g. MIL-53 and MOF-508b); (b) subnetwork displacement (e.g. MOF-508b). These result in a stepped isotherm (c), due to the structural transitions between the narrow pore (np) and large pore (lp) forms.[10,23,24]

[a] W. K. Feldmann, Prof. C. Esterhuysen, Prof. L. J. Barbour
Department of Chemistry and Polymer Science
University of Stellenbosch, Matieland 7600 (South Africa)
E-mail: ljb@sun.ac.za
Homepage: http://academic.sun.ac.za/barbour/

Supporting information for this article is available on the WWW under https://doi.org/10.1002/cssc.202001469

the events that usually occur when flexible materials transform in response to gas uptake and release. Indeed, few studies have employed calorimetric methods to investigate the adsorption enthalpies of flexible materials over a wide pressure range.[27,28] Most notable is the well-known metal-organic framework (MOF) MIL-53(Al)[29] (see the Supporting Information, Table S5),[30–32] rendering it a suitable reference compound for validation of our results. It has been noted that MIL-53(Al) exists in a large pore (lp) form when completely activated but upon exposure to CO_2, even at low loading, it immediately contracts to a narrow pore (np) form. This is unusual as flexible materials generally collapse to the np form upon complete guest removal. At higher CO_2 loadings it then reverts to the lp form through a breathing mode structural transition (Figure 1a).[22] MOF-508b[33,34] exhibits two structural transitions, primarily subnetwork displacement followed by a secondary breathing mode (Figure 1a and b), which adds additional complexity.

Using a modification of our reported PG-DSC procedure,[25] we determined the enthalpies of CO_2 adsorption and desorption for both MIL-53(Al) and MOF-508b at 288, 298 and 308 K in the context of thermal management; the isotherms are shown in blue in Figures 2 and 3. In addition to the expected stepped profiles, the isotherms display considerable hysteresis.[35] These were determined for the narrow (np) and large pore (lp) forms,

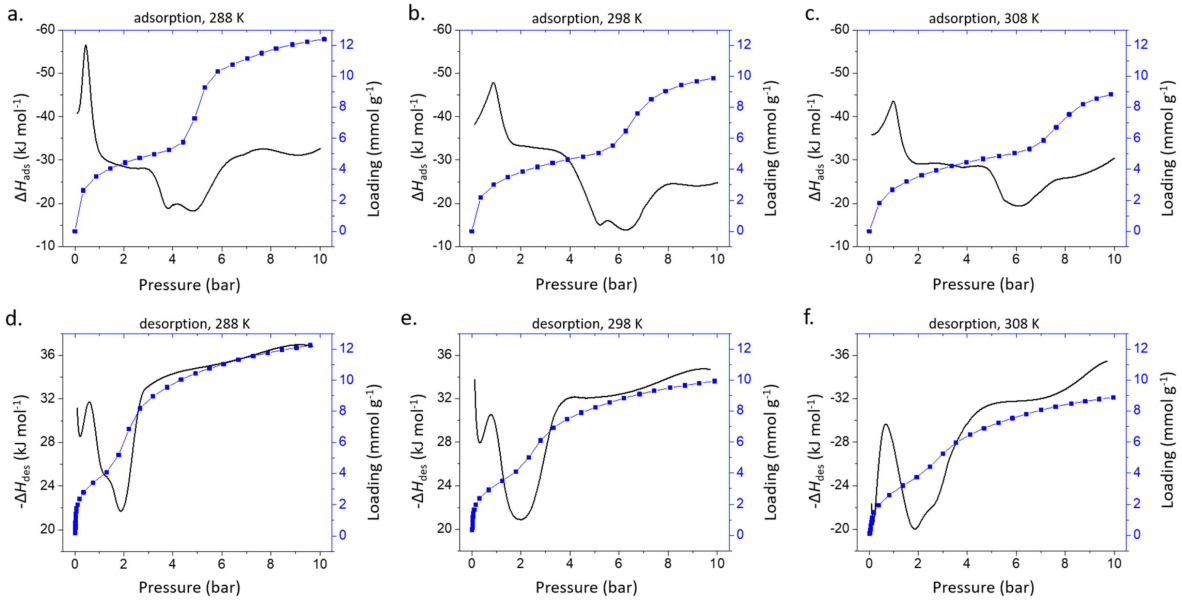

Figure 2. Differential enthalpy plots overlaid with the corresponding sorption isotherms for MIL-53(Al).

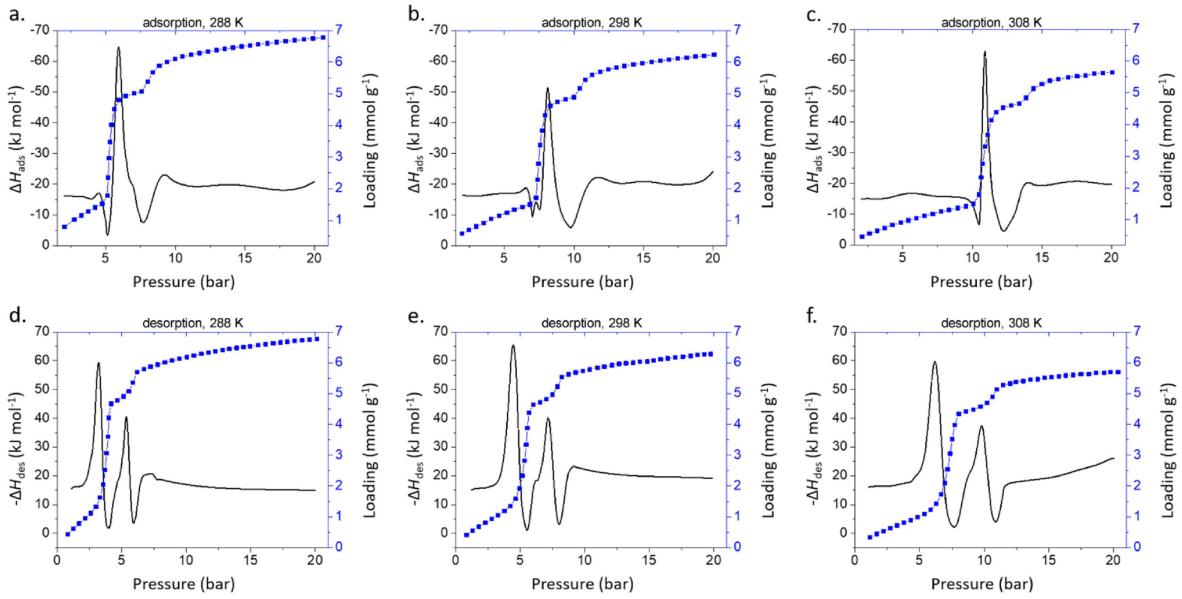

Figure 3. Differential enthalpy plots overlaid with the corresponding sorption isotherms for MOF-508b.

associated with the structural transition. Previously reported $-\Delta H_{ads}$ values for the (np) and (lp) forms of MIL-53(Al) (i.e., before and after the structural transition) span the ranges 24 to 50 and 15 to 26 kJ mol^{-1}, respectively (Table S5). Our results for the np and lp pore forms span 28 to 32 and 14 to 19 kJ mol^{-1}, respectively, agreeing well within the established adsorption ranges.

The differential enthalpy profiles for the adsorption of CO_2 at each temperature by MIL-53(Al) are shown in black in Figure 2. In accordance with the sorption isotherms, each plot shows two distinct regions, each consisting of one or more thermal events. The first adsorption region ranges from zero loading to the onset of the np → lp structural expansion at approximately 4, 5 or 6 bar, depending on the temperature. The exothermic process between 0 and 1 bar is due to initial guest adsorption, involving the unusual lp→np structural contraction around the guest molecules.[5] The subsequent endothermic region is related to the np→lp structural expansion, followed by exothermic guest adsorption into the lp phase. The endo- and exothermic contributions can be observed, which is valuable when assessing the thermal properties of the material.

Desorption and the related hysteresis profiles are rarely investigated for thermal effects, which is surprising considering that the deliverability of a guest is directly related to desorption and the corresponding enthalpy. The differential enthalpy plots for desorption (Figure 2d–f) exhibit trends that match those for adsorption, albeit with hysteresis and in the opposing thermal direction, i.e. an exotherm in the adsorption profile corresponds to an endotherm in the desorption profile. The differential enthalpies for the exothermic lp→np structural contraction and the endothermic guest desorption are consistent over the three temperatures, showing a decrease in enthalpy, which leads to cooling of the system in the pressure region of the structural transition.

Figure 2 describes how the differential enthalpy changes over a given pressure range. These plots offer valuable information for application-based assessment of adsorbent materials, enabling one to monitor the thermal characteristics at a given pressure. Using this approach, adsorbent materials can be benchmarked against one another to determine the ideal adsorbent for a specific gas over a specific pressure range in terms of their thermal phenomena. Additionally, these types of plots can provide insights that are useful for management of the thermal changes within the system. For example, more heat is evolved between 0–5 bar than between 5–10 bar when MIL-53(Al) adsorbs CO_2.

Such information can be used to formulate a cooling profile to maintain the system at ideal conditions for maximum performance.

MOF-508b is a more complex flexible system, exhibiting two structural expansions (subnetwork displacement: np↔lp and breathing: lp↔2lp) that result in two-stepped profiles for both adsorption and desorption (Figure 3, blue). The material initially exhibits a sharp endotherm corresponding to sub-network displacement. However, the magnitudes of the subsequent adsorption exotherms are exceptionally high, with peak values of ca −64.7, −51.5 and −63.0 kJ mol^{-1} at 288, 298 and 308 K, respectively (Figure 3a–c). This suggests that strong host-guest interactions occur rapidly subsequent to the np→lp expansion, which is further corroborated by the corresponding steep gradients of the isotherms. The secondary structural expansion (lp→2lp) is challenging to interpret as the onset of the transition overlaps with the preceding large exotherm. However, the enthalpy thereafter is greatly reduced in comparison to the first exotherm, suggesting that the different modes of flexibility may exhibit different enthalpy profiles (it would be interesting to see if future studies can confirm that this is generally applicable for flexible systems). Summing the energies associated with the initial np→lp endotherm and subsequent exotherm yields −47.5, −32.6 and −47.3 kJ mol^{-1} at 288, 298 and 308 K, respectively. This is a clear indication that the exothermic adsorption enthalpy far exceeds that of the endotherm associated with the structural transition. During desorption the exotherm corresponding to the transition 2lp→lp is considerably more pronounced than the endotherm for the reverse process, indicating strong host-guest interactions and potential guest trapping.[36] This results in a different thermal pathway to remove the guest from the host material.

Integrating the enthalpy profiles with respect to loading yields the total enthalpy for the entire sorption process. Both materials were compared to a hypothetical rigid framework to assess the magnitude of the enthalpy offset due to structural flexibility (e.g., Figure 4, and Tables S1–S4 in the Supporting Information).[2] MIL-53(Al) shows a reduction in the total enthalpy of ca 8% to 18% as compared to the rigid framework for both adsorption and desorption at all three temperatures investigated. Similar results were obtained for MOF-508b at the two higher temperatures, but a net gain in enthalpy was observed at 288 K. This result for MOF-508b implies that, by judicial selection of the temperature, it is possible that enthalpic structural transitions by flexible materials can be utilized to mitigate heating resulting from sorption processes.

For the purposes of comparison, the enthalpy profiles indicate that MIL-53(Al) would perform better than MOF-508b as an adsorbent for CO_2 sorption. This is due to the balance between the endo- and exotherms shown in the differential plots and a reduction in total integral enthalpy over the entire pressure range investigated for both adsorption and desorption. MOF-508b shows the potential for a similar heat reduction, however the large and rapid generation of enthalpy displayed

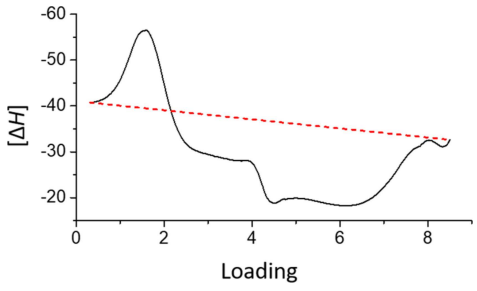

Figure 4. A comparison between the differential enthalpy plot (black line) for MIL-53(Al) at 288 K and a hypothetical rigid framework (dashed line). Integrating the area under each curve yields the total integral heat associated with the entire sorption process.

in the differential plots would be detrimental for sorbent applications. Advanced external cooling would be required to maintain optimal working conditions for such a flexible system.

In conclusion, we have devised a scanning calorimetric method to continuously measure the energetic profiles for gas adsorption and release by flexible porous materials. The high-resolution plots of differential enthalpy vs. pressure offer comprehensive insight into enthalpy changes over the entire working range for sorption processes. The compounds studied here show an overall reduction in the total integral enthalpy associated with adsorption relative to that obtained for rigid materials. We have shown that it is necessary to assess both differential and integral enthalpy values when evaluating the thermal behaviour of flexible materials. Such assessments offer crucial information that ultimately aids in the development and evaluation of new and existing materials to increase energy efficiency and optimize gas storage capacities.

Experimental Section

The materials MIL-53(Al) and MOF-508b were synthesized according to well-established reported procedures.[29,33] The sorption experiments were conducted using a Hy-Energy PCTPro-2000 equipped with a Microdoser module. A Grant refridgerated bath was used to thermostat the sample chamber. The energetic measurements were recorded using a Setaram μDSC7 Evo module equipped with a high pressure sample holder. The pressure gradient was controlled by means of a ProportionAir QPV1 M pressure valve.

Acknowledgements

We thank the National Research Foundation of South Africa for funding this work.

Conflict of Interest

The authors declare no conflict of interest.

Keywords: adsorption · calorimetry · enthalpies · metal-organic frameworks · porous materials

[1] K. J. Chang, O. Talu, *Appl. Therm. Eng.* **1996**, *16*, 359.
[2] J. A. Mason, J. Oktawiec, M. K. Taylor, M. R. Hudson, J. Rodriguez, J. E. Bachman, M. I. Gonzalez, A. Cervellino, A. Guagliardi, C. M. Brown, P. L. Llewellyn, N. Masciocchi, J. R. Long, *Nature* **2015**, *527*, 357.
[3] S. Sircar, *Ind. Eng. Chem. Res.* **2006**, *45*, 5435.
[4] B. Mu, F. Li, Y. Huanga, K. S. Walton, *J. Mater. Chem.* **2012**, *22*, 10172.
[5] A. Boutin, F.-X. Coudert, M.-A. Springuel-Huet, A. V. Neimark, G Férey, A. H. Fuchs, *J. Phys. Chem. C* **2010**, *114*, 22237.
[6] P. L. Llewellyn, G. Maurin, *C. R. Chim.* **2005**, *8*, 283.
[7] Y. Park, Y. Ju, D. Park, C.-H. Lee, *Chem. Eng. J.* **2016**, *292*, 348.
[8] J. Moellmer, A. Moeller, F. Dreisbach, R. Glaeser, R. Staudt, *Microporous Mesoporous Mater.* **2011**, *138*, 140.
[9] N. Bimbo, J. E. Sharpe, V. P. Ting, A. Noguera-Díaz, T. J. Mays, *Adsorption* **2014**, *20*, 373.
[10] Q.-Y. Yang, P. Lama, S. Sen, M. Lusi, K.-J. Chen, W.-Y. Gao, M. Shivanna, T. Pham, N. Hosono, S. Kusaka, J. J. Perry, S. Ma, B. Space, L. J. Barbour, S. Kitagawa, M. J. Zaworotko, *Angew. Chem. Int. Ed.* **2018**, *57*, 5684; *Angew. Chem.* **2018**, *130*, 5786.
[11] M. K. Taylor, T. Runčevski, J. Oktawiec, J. E. Bachman, R. L. Siegelman, H. Jiang, J. A. Mason, J. D. Tarver, J. R. Long, *J. Am. Chem. Soc.* **2018**, *140*, 10324.
[12] C. M. McGuirk, T. Runčevski, J. Oktawiec, A. Turkiewicz, M. K. Taylor, J. R. Long, *J. Am. Chem. Soc.* **2018**, *140*, 15924.
[13] H. Pan, J. A. Ritter, P. B. Balbuena, *Langmuir* **1998**, *14*, 6323.
[14] Y. Tian, J. Wu, *Langmuir* **2017**, *33*, 996.
[15] M. M. K. Salem, P. Braeuer, M. v. Szombathely, M. Heuchel, P. Harting, K. Quitzsch, *Langmuir* **1998**, *14*, 3376.
[16] A. Chakraborty, B. B. Saha, S. Koyama, K. C. Ng, *Appl. Phys. Lett.* **2006**, *89*, 171901.
[17] R. P. P. L. Ribeiro, B. C. R. Camacho, A. Lyubchyk, I. A. A. C. Esteves, F. J. A. L. Cruz, J. P. B. Mota, *Microporous Mesoporous Mater.* **2016**, *230*, 154.
[18] S. Hiraide, H. Tanaka, N. Ishikawa, M. T. Miyahara, *ACS Appl. Mater. Interfaces* **2017**, *9*, 41066.
[19] S. Krause, J. D. Evans, V. Bon, I. Senkovska, S. Ehrling, U. Stoeck, P. G. Yot, P. Iacomi, P. Llewellyn, G. Maurin, F.-X. Coudert, S. Kaskel, *J. Phys. Chem. C* **2018**, *122*, 19171.
[20] F.-X. Coudert, M. Jeffroy, A. H. Fuchs, A. Boutin, C. Mellot-Draznieks, *J. Am. Chem. Soc.* **2008**, *130*, 14294.
[21] F. Rouquerol, J. Rouquerol, K. S. W. Sing, P. Llewellyn, G. Maurin, *Adsorption by Powders and Porous Solids*, Academic Press, London, **2014**.
[22] A. Schneemann, V. Bon, I. Schwedler, I. Senkovska, S. Kaskel, R. A. Fischer, *Chem. Soc. Rev.* **2014**, *43*, 6062.
[23] K. S. W. Sing, D. H. Everett, R. A. W. Haul, L. Moscou, R. A. Pierotti, J. Rouquerol, T. Siemieniewska, *Pure* **1985**, *57*, 603.
[24] S. Brunauer, L. S. Deming, W. E. Deming, E. Teller, *J. Am. Chem. Soc.* **1940**, *62*, 1723.
[25] W. K. Feldmann, K.–A. White, C. X. Bezuidenhout, V. J. Smith, C. Esterhuysen, L. J. Barbour, *ChemSusChem* **2020**, *13*, 102.
[26] J. Rouquerol, S. Partyka, F. Rouquerol, *J. Chem. Soc. Faraday Trans.* **1977**, *73*, 306.
[27] P. Iacomi, B. Zheng, S. Krause, S. Kaskel, G. Maurin, P. L. Llewellyn, *Chem. Mater.* **2020**, *32*, 3489.
[28] J. Rodriguez, I. Beurroies, M.-V. Coulet, P. Fabry, T. Devic, C. Serre, R. Denoyela, P. L. Llewellyn, *Dalton Trans.* **2016**, *45*, 4274.
[29] T. Loiseau, C. Serre, C. Huguenard, G. Fink, F. Taulelle, M. Henry, T. Bataille, G. Férey, *Chem. Eur. J.* **2004**, *10*, 1373.
[30] S. Bourrelly, P. L. Llewellyn, C. Serre, F. Millange, T. Loiseau, G. Férey, *J. Am. Chem. Soc.* **2005**, *127*, 13519.
[31] N. A. Ramsahye, G. Maurin, S. Bourrelly, P. Llewellyn, T. Loiseau, G. Férey, *Phys. Chem. Chem. Phys.* **2007**, *9*, 1059.
[32] E. Dundar, N. Chanut, F. Formalik, P. Boulet, P. L. Llewellyn, B. Kuchta, *J. Mol. Modeling* **2017**, *23*, 101.
[33] B. Chen, C. Liang, J. Yang, D. S. Contreras, Y. L. Clancy, E. B. Lobkovsky, O. M. Yaghi, S. Dai, *Angew. Chem. Int. Ed.* **2006**, *45*, 1390; *Angew. Chem.* **2006**, *118*, 1418.
[34] P. M. Bhatt, E. Batisai, V. J. Smith, L. J. Barbour, *Chem. Commun.* **2016**, *52*, 11374.
[35] S. A. Sapchenko, M. O. Barsukova, R. V. Belosludov, K. A. Kovalenko, D. G. Samsonenko, A. S. Poryvaev, A. M. Sheveleva, M. V. Fedin, A. S. Bogomyakov, D. N. Dybtsev, M. Schröder, V. P. Fedin, *Inorg. Chem.* **2019**, *58*, 6811.
[36] H. Bunzen, F. Kolbe, A. Kalytta-Mewes, G. Sastre, E. Brunner, D. Volkmer, *J. Am. Chem. Soc.* **2018**, *140*, 10191.

Manuscript received: June 14, 2020
Revised manuscript received: August 17, 2020
Accepted manuscript online: August 23, 2020
Version of record online: September 9, 2020